

# Balance of an inverted pendulum on a drone with a MPC controller

Claudio Anzalone, Paolo Maisto, Antonio Manzoni, Gaetano Parigiano, Angelo Vittozzi

**Abstract**—In this paper, the aim is to balance an inverted pendulum mounted on a quadrotor aerial vehicle using a Model Predictive Control (MPC) controller by computational modeling and simulation. Static and dynamic modeling of the system are studied to find nominal states of the system at standstill and on circular trajectories. Control laws are designed around these nominal trajectories. It is considered a yaw-independent quadrotor dynamic. It is introduced a ‘Virtual Body Frame’ that allows time-invariant description of the trajectories. For implementation and results visualization, it has been used Matlab environment. A development for the future is focused on the simulation in a real environment.

**Index Terms**—quadcopter, inverted pendulum, MPC, Matlab

## I. INTRODUCTION

In this paper, the system in analysis is composed by two subsystems: quadcopter and inverted pendulum. In first, the focus was on the modelling of these two subsystems in a separately way and then on the combined model of the system.

It is developed a MPC control strategy that at the same time balances an inverted pendulum on top of a quadrotor and allows trajectory tracking. The main reason to use MPC is the ability to consider control and state constraints that occur in practical problems [3]. In addition, MPC can provide better performance than other traditional control methods.

Tests and results visualization are implemented through the simulation tool made available by Matlab. For the MPC’s optimization problem it is used CVX, a Matlab-based modeling system for convex optimization.

In Section II, it is introduced the dynamic models used in the controller design. Section III presents static and dynamic nominal trajectories for the quadrotor to follow. The dynamics are then linearized around these trajectories in Section IV, and linear state feedback controllers are designed in Section V. The simulation results are shown in Section VI and conclusions are drawn in Section VII, where an outlook is also presented.

## II. DYNAMICS

The equations of motion are obtained for both the quadrotor and the inverted pendulum, considering the general case that is not dependent on any specific trajectory.

Considering the significant difference in mass between the pendulum and the quadrotor, it is reasonable to assume that the reactive forces exerted by the pendulum on the quadrotor can be neglected.

As a result, the dynamics of the quadrotor are independent of the pendulum, while the motion of the quadrotor affects the dynamics of the pendulum.

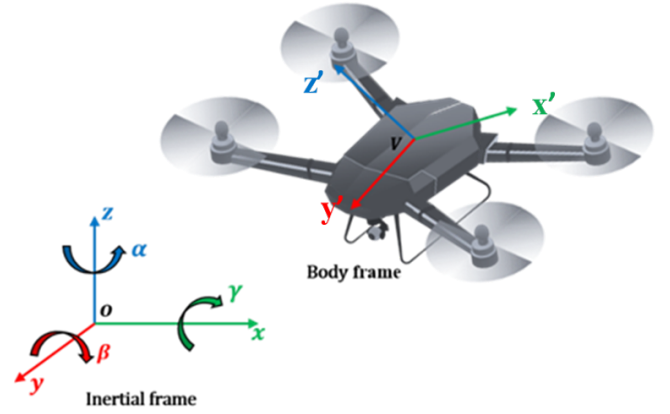


Figure 1: The inertial coordinate system O and the vehicle coordinate system V.

### A. Quadrotor

The quadrotor is characterized by six degrees of freedom: the quadrotor’s position in space  $(x, y, z)$  is measured in the inertial frame O as shown in Figure 1. The orientation of the quadrotor, referred to as vehicle attitude V, is defined by three Euler angles. In particular, it is used the Euler angles convention Roll-Pitch-Yaw (RPY). This one is used usually in aeronautics field to describe the three-dimensional orientation of aerial vehicles. This convention is the only one that adopts a sequence of rotations that take place in fixed frame. From the last one, the rotation is carried out around the x-axis by the roll angle  $\gamma$ . The coordinate system is then rotated around the new y-axis by the pitch angle  $\beta$ , and finally rotated about the new z-axis by the yaw angle  $\alpha$ , so the rotation matrix is:

$$R_V^O(\alpha, \beta, \gamma) = R_z(\alpha)R_y(\beta)R_x(\gamma) \quad (1)$$

where

$$R_x(\gamma) = \begin{bmatrix} 1 & 0 & 0 \\ 0 & \cos(\gamma) & -\sin(\gamma) \\ 0 & \sin(\gamma) & \cos(\gamma) \end{bmatrix} \quad (2)$$

$$R_y(\beta) = \begin{bmatrix} \cos(\beta) & 0 & \sin(\beta) \\ 0 & 1 & 0 \\ -\sin(\beta) & 0 & \cos(\beta) \end{bmatrix} \quad (3)$$

$$R_z(\alpha) = \begin{bmatrix} \cos(\alpha) & -\sin(\alpha) & 0 \\ \sin(\alpha) & \cos(\alpha) & 0 \\ 0 & 0 & 1 \end{bmatrix} \quad (4)$$

The translational acceleration of the vehicle is determined by the vehicle’s attitude and the total thrust generated by the four motors.

Denoting the collective thrust as  $a$ , the translational acceleration in the inertial frame can be expressed as follows:

$$\begin{bmatrix} \ddot{x} \\ \ddot{y} \\ \ddot{z} \end{bmatrix} = R_V^O(\alpha, \beta, \gamma) \begin{bmatrix} 0 \\ 0 \\ a \end{bmatrix} + \begin{bmatrix} 0 \\ 0 \\ -g \end{bmatrix} \quad (5)$$

The control inputs are the desired rotational rates about the vehicle body axes,  $(\omega_x, \omega_y, \omega_z)$ , and the collective thrust  $a$ .

Quadrotor's motors can produce very high torques, it is due to the very low rotational inertia, in fact they can reach rotational accelerations of about 200 rad/s<sup>2</sup>.

In this project it is considered as hypothesis that the quadrotor has a fast response time to in the desired rotational rate changes requested by control strategy. We will therefore assume that it can directly control the vehicle body rates and ignore rotational acceleration dynamics. As with the quadrotor body rates, also the thrust can be changed instantaneously.

The rates of the Euler angles are converted to the quadrotor body frame V through their respective transformations:

$$\begin{bmatrix} \omega_x \\ \omega_y \\ \omega_z \end{bmatrix} = R_x(\gamma)R_y(\beta) \begin{bmatrix} 0 \\ 0 \\ \dot{\alpha} \end{bmatrix} + R_z(\alpha) \begin{bmatrix} 0 \\ \dot{\beta} \\ 0 \end{bmatrix} + \begin{bmatrix} \dot{\gamma} \\ 0 \\ 0 \end{bmatrix} \quad (6)$$

The above can be written more compactly by combining the Euler rates into a single vector, calculating the relevant rows of the rotation matrices, and solving for the Euler angle rates:

$$\begin{bmatrix} \dot{\gamma} \\ \dot{\beta} \\ \dot{\alpha} \end{bmatrix} = \begin{bmatrix} 1 & 0 & \sin(\beta) \\ 0 & \cos(\gamma) & -\cos(\gamma)\sin(\gamma) \\ 0 & \sin(\gamma) & \cos(\beta)\cos(\gamma) \end{bmatrix} \begin{bmatrix} \omega_x \\ \omega_y \\ \omega_z \end{bmatrix} \quad (7)$$

### B. Inverted Pendulum

The pendulum has two degrees of freedom, which are described by the translational position of the pendulum centre of mass relative to its base in O ( $r$  along the x-axis,  $s$  along the y-axis). For notational simplicity, it is described the relative position of the pendulum along the z-axis as:

$$\zeta := \sqrt{L^2 - r^2 - s^2} \quad (8)$$

where  $L$  denotes the length from the base of the pendulum to its center of mass. The pendulum is modelled as a mass that is rigidly attached to the mass center of the quadrotor, such that rotations of the vehicle do not cause a motion of the pendulum base. A Lagrangian approach was used to explain the pendulum equations. The Lagrangian of the pendulum can be written as

$$\mathcal{L} := \frac{1}{2} \left( (\dot{x} + \dot{r})^2 + (\dot{y} + \dot{s})^2 + \left( \dot{z} - \frac{r\dot{r} + s\dot{s}}{\zeta} \right)^2 \right) - g(z + \zeta) \quad (9)$$

It was assumed that the mass of the pendulum is unitary, without loss of generality. The first term represents the kinetic energy of the pendulum, and the second the potential energy. By using the Lagrangian formulae, it is possible to obtain the Euler-Lagrange equations, which are differential equations that describe the system's motion. These equations allow to determine the trajectories and laws of motion of the system, providing an accurate mathematical description of mechanical behavior:

$$\frac{d}{dt} \left( \frac{\partial \mathcal{L}}{\partial \dot{r}} \right) - \frac{\partial \mathcal{L}}{\partial r} = 0 \quad (10)$$

$$\frac{d}{dt} \left( \frac{\partial \mathcal{L}}{\partial \dot{s}} \right) - \frac{\partial \mathcal{L}}{\partial s} = 0 \quad (11)$$

These equations could be embedded in a more compact form:

$$\begin{bmatrix} \ddot{r} \\ \ddot{s} \end{bmatrix} = f(r, s, \dot{r}, \dot{s}, \ddot{x}, \ddot{y}, \ddot{z}) \quad (12)$$

where  $f$  are the nonlinear equations (13) and (14).

$$\begin{aligned} \ddot{r} = & \frac{1}{(L^2 - s^2)\zeta^2} \left( -r^4 \ddot{x} - (L^2 - s^2) \ddot{x} - 2r^2 (s\dot{r}\dot{s} + (-L^2 + s^2) \ddot{x}) + \right. \\ & + r^3 (\dot{s}^2 + s\ddot{s} - \zeta(g + \ddot{z})) + r (-L^2 s\ddot{s} + s^3 \ddot{s} + s^2 (\dot{r}^2 - \zeta(g + \ddot{z}))) \\ & \left. + L^2 (-\dot{r}^2 - \dot{s}^2 + \zeta(g + \ddot{z})) \right) \end{aligned} \quad (13)$$

$$\begin{aligned} \ddot{s} = & \frac{1}{(L^2 - r^2)\zeta^2} \left( -s^4 \ddot{y} - (L^2 - r^2) \ddot{y} - 2s^2 (r\dot{r}\dot{s} + (-L^2 + r^2) \ddot{y}) + \right. \\ & + s^3 (\dot{r}^2 + r\ddot{r} - \zeta(g + \ddot{z})) + s (-L^2 r\ddot{r} + r^3 \ddot{r} + r^2 (\dot{s}^2 - \zeta(g + \ddot{z}))) \\ & \left. + L^2 (-\dot{r}^2 - \dot{s}^2 + \zeta(g + \ddot{z})) \right) \end{aligned} \quad (14)$$

### C. Combined dynamics

The equations (5), (7), and (12) completely describe the dynamics of the combined system. The attitude V of the vehicle is controlled in a nonlinear manner by the three body rate control inputs  $(\omega_x, \omega_y, \omega_z)$ . This attitude, combined with the thrust  $a$ , controls the translational acceleration of the vehicle. By adjusting the thrust parameter  $a$ , the translational acceleration of the vehicle is controlled. This acceleration governs the linear motion of the vehicle while simultaneously influencing the pendulum's motion through nonlinear equations.

The combined system consists of thirteen states (three rotational and six translational states of the quadrotor, and four states of the pendulum), and four control inputs (three body rotational rates, and the thrust).

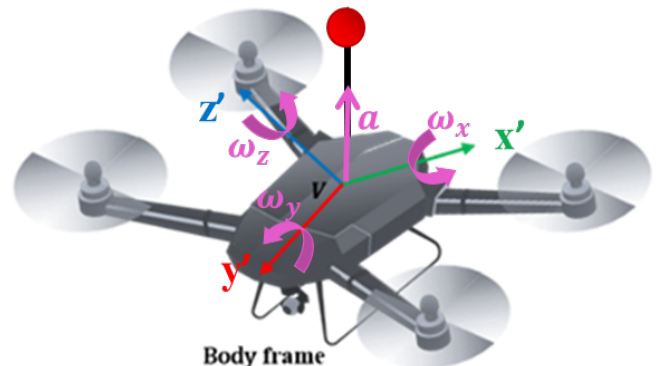


Figure 2: The control inputs of the quadrotor: the rotational rates  $\omega_x$ ,  $\omega_y$ ,  $\omega_z$  and the total thrust  $a$ .

### III. NOMINAL TRAJECTORIES

In this section, we find static and dynamic equilibria of the system that meet the conditions outlined in Equations (5), (7), and (12). These equilibria serve as nominal trajectories to be tracked by the quadrotor. Corresponding control inputs associated with these nominal trajectories are also detailed. For convenience, we denote these nominal values with a zero index ( $x_0$ ,  $r_0$ , etc.).

#### A. Constant position

In a first case, we require  $x_0$ ,  $y_0$ , and  $z_0$  to be constant. Substituting these constraints into equation (5) the first term is a zero vector because there are derivatives of constant parameters. We observe that  $\beta_0 = 0$  and  $\gamma_0 = 0$  satisfy the equations when  $a_0 = g$ . The parameter  $\alpha_0$  can be chosen arbitrarily. In this case, it was assumed that  $\alpha_0 = 0$ . Using the given angles ( $\alpha_0$ ,  $\beta_0$ ,  $\gamma_0$ ), equation (7) can be solved with the body rate control inputs being  $w_{x_0} = w_{y_0} = w_{z_0} = 0$ . Inserting the nominal states ( $x_0$ ,  $y_0$ ,  $z_0$ ) into the pendulum equations of motion (12), they simplify to:

$$\ddot{r} = r \frac{g\zeta^3 - L^2(\dot{r}^2 + \dot{s}^2) + (s\dot{r} - r\dot{s})^2}{L^2\zeta^2} \quad (15)$$

$$\ddot{s} = s \frac{g\zeta^3 - L^2(\dot{r}^2 + \dot{s}^2) + (s\dot{r} - r\dot{s})^2}{L^2\zeta^2} \quad (16)$$

These equations are solved by the static equilibrium:

$$r = r_0 = 0 \quad (17)$$

$$s = s_0 = 0 \quad (18)$$

meaning that, as expected, the inverted pendulum is exactly over the quadrotor.

#### B. Circular trajectory

As a second nominal trajectory, we specify that the quadrotor must follow a circular path with a predetermined radius  $R$  while maintaining a constant rotational rate  $\Omega$  and altitude  $z_0$ . To achieve this, we aim to convert the equations of motion into alternative coordinate systems such that the nominal states and the linearized dynamics about them can be described in a time-invariant manner. A virtual frame is a coordinate system than is independent from the time, but it is based on the pose (position and orientation) of the quadrotor in the space.

To describe the vehicle position, the following coordinate system C is introduced, with  $(u, v, w)$  describing the position in C:

$$\begin{bmatrix} x \\ y \\ z \end{bmatrix} := R_z(\Omega t) \begin{bmatrix} u \\ v \\ w \end{bmatrix} = \begin{bmatrix} \cos \Omega t & -\sin \Omega t & 0 \\ \sin \Omega t & \cos \Omega t & 0 \\ 0 & 0 & 1 \end{bmatrix} \begin{bmatrix} u \\ v \\ w \end{bmatrix} \quad (19)$$

To represent the vehicle's attitude, we introduce an additional set of Euler angles, which describe the 'virtual body frame' W. These angles are denoted as  $\eta$ ,  $\mu$ , and  $\nu$ :

$$R_W^O R(\eta, \mu, \nu) = R_z(\eta) R_y(\mu) R_x(\nu) \quad (20)$$

subject to the constraint that

$$R_V^O R(\alpha, \beta, \gamma) \begin{bmatrix} 0 \\ 0 \\ 1 \end{bmatrix} = R_W^O R(\eta, \mu, \nu) \begin{bmatrix} 0 \\ 0 \\ 1 \end{bmatrix} \quad (21)$$

The above equation provides values for three elements of the rotation matrices. As every column of a rotation matrix has unit norm, however, this equation only defines two of the angles ( $\eta$ ,  $\mu$ ,  $\nu$ ). By comparing the constraint (21) with the translational equation of motion of the vehicle (5), it becomes apparent that the virtual body frame W represents an attitude constrained in such a way that it induces the same translational motion in the quadrotor as the vehicle attitude V. The remaining degree of freedom represents the fact that rotations about the z-axis along which  $\omega_z$  acts have no effect on the quadrotors translational motion. Applying (19), its derivatives, (19), and setting the free parameter  $\eta = \Omega t$ , the quadrotor equation of motion (5) simplifies to

$$\begin{bmatrix} \ddot{u} \\ \ddot{v} \\ \ddot{w} \end{bmatrix} = \begin{bmatrix} a \sin \mu \cos \nu + \Omega^2 u + 2\Omega \dot{v} \\ -a \sin \nu - 2\Omega \dot{u} + \Omega^2 v \\ a \cos \mu \cos \nu - g \end{bmatrix} \quad (22)$$

The circular trajectory is described by  $u_0 = R$ ,  $v_0 = 0$ , and  $\dot{w}_0 = 0$ . Using these values, the nominal Euler angles  $\mu_0$  and  $\nu_0$ , as well as the nominal thrust  $a_0$  can be computed:

$$\mu_0 = \arctan\left(-\frac{\Omega^2 R}{g}\right) \quad (23)$$

$$\nu_0 = 0 \quad (24)$$

$$a_0 = \sqrt{g^2 + (\Omega^2 R)^2} \quad (25)$$

Given the nominal values for  $(\eta_0, \mu_0, \nu_0)$ , we can determine the corresponding values for  $(\alpha_0, \beta_0, \gamma_0)$  by solving Equation (21). Similar to the scenario of constant position, we set  $\alpha_0 = 0$ , resulting in the simplification of Equation (21) to

$$\begin{bmatrix} \sin \beta_0 \cos \gamma_0 \\ -\sin \gamma_0 \\ \cos \beta_0 \cos \gamma_0 \end{bmatrix} = \begin{bmatrix} \cos \Omega t \sin \mu_0 \cos \nu_0 + \sin \Omega t \sin \nu_0 \\ \sin \Omega t \sin \mu_0 \cos \nu_0 - \cos \Omega t \sin \nu_0 \\ \cos \mu_0 \cos \nu_0 \end{bmatrix} \quad (26)$$

which can be solved for  $\beta_0$  and  $\gamma_0$ . With this, the description of the required nominal states for the translational motion (5) is complete. In both coordinate systems C and W, the nominal position and attitude remain constant. By utilizing Equations (19) and (26), the time-varying nominal states in O and V can be determined. In order to compute the rotational rate control inputs in Equation (7), we differentiate Equation (26). It can be demonstrated that:

$$\dot{\beta}_0 = \frac{R\Omega^3 \cos^{-1} \gamma_0 (\tan \beta_0 \tan \gamma_0 \cos(\Omega t) + \cos^{-1} \beta_0 \sin(\Omega t))}{\sqrt{g^2 + (\Omega^2 R)^2}} \quad (27)$$

$$\dot{\gamma}_0 = \frac{R\Omega^3 \cos^{-1} \gamma_0 \cos(\Omega t)}{\sqrt{g^2 + (\Omega^2 R)^2}} \quad (28)$$

By combining these equations with the outcomes derived from Equations (26) and (7), it becomes possible to determine the nominal states corresponding to the nominal control inputs  $(\omega_{x_0}, \omega_{y_0}, \omega_{z_0})$ .

Like the vehicle, the pendulum's relative coordinates  $r$  and  $s$  are subject to rotation by  $\Omega t$ .

$$\begin{bmatrix} r \\ s \end{bmatrix} := \begin{bmatrix} \cos \Omega t & -\sin \Omega t \\ \sin \Omega t & \cos \Omega t \end{bmatrix} \begin{bmatrix} p \\ q \end{bmatrix} \quad (29)$$

By applying this rotation to the Lagrangian formulations describing the motion of the pendulum (10) and (11), while setting the base motion  $(\ddot{x}, \ddot{y}, \ddot{z})$  as the circular trajectory, it can be demonstrated that the dynamics of the pendulum can be expressed as follows:

$$\begin{aligned} p \left( \frac{p\ddot{p} + \dot{p}^2 + q\ddot{q} + \dot{q}^2}{\zeta^2} + \frac{q^2\dot{q}^2 + p^2\dot{p}^2 + 2pq\dot{p}\dot{q}}{\zeta^4} - \frac{g}{\zeta} - \Omega^2 \right) \\ + \ddot{p} - 2\Omega\dot{q} - R\Omega^2 = 0 \end{aligned} \quad (30)$$

$$\begin{aligned} q \left( \frac{q\ddot{q} + \dot{q}^2 + p\ddot{p} + \dot{p}^2}{\zeta^2} + \frac{p^2\dot{p}^2 + 2pq\dot{p}\dot{q} + q^2\dot{q}^2}{\zeta^4} - \frac{g}{\zeta} - \Omega^2 \right) \\ + \ddot{q} + 2\Omega\dot{p} = 0 \end{aligned} \quad (31)$$

We aim to find a solution where  $\dot{p}_0, \dot{q}_0, \ddot{p}_0, \ddot{q}_0$  are all equal to zero. This results in the following constraints for equilibrium points:

$$\Omega^2(q_0) + \frac{gq_0}{\zeta_0} = 0 \quad (32)$$

$$\Omega^2(R + q_0) + \frac{gp_0}{\zeta_0} = 0 \quad (33)$$

The first equation indicates that the only solution is  $q_0 = 0$ . The second equation establishes a nonlinear relationship among  $\Omega$ ,  $R$ , and  $p_0$ . There is always a solution for  $p_0$  within the range of  $-R \leq p_0 \leq 0$ . This result flows into intuition: the center of mass of the pendulum must be positioned towards the center of the circle to ensure that the centripetal force exerted on it is balanced by gravity. If the center of mass were located farther inwards than  $R$ , the centripetal force would change direction and sign, causing the pendulum to fall.

#### IV. DYNAMICS ABOUT NOMINAL TRAJECTORIES

The linear approximations of the dynamics are obtained by performing a first-order Taylor expansion of the equations of motion (5), (7), and (12) around the nominal trajectories determined in Section III. To denote small deviations, we use the tilde symbol  $(\tilde{x}, \tilde{r}, \text{etc.})$ . In this paper, we present only the resulting linearized dynamics.

##### A. Constant position

Under the assumption of a constant nominal position and zero yaw angle, the translational degrees of freedom in the quadrotor-pendulum system can be completely decoupled along the three axes of the O coordinate system. This decoupling yields the following equations:

$$\ddot{\tilde{r}} = \tilde{r} \frac{g}{L} - \tilde{\beta} g \quad (34)$$

$$\ddot{\tilde{s}} = \tilde{s} \frac{g}{L} + \tilde{\gamma} g \quad (35)$$

$$\ddot{\tilde{x}} = \tilde{\beta} g \quad (36)$$

$$\ddot{\tilde{y}} = -\tilde{\gamma} g \quad (37)$$

$$\dot{\tilde{\beta}} = \tilde{\omega}_y \quad (38)$$

$$\dot{\tilde{\gamma}} = \tilde{\omega}_x \quad (39)$$

$$\ddot{\tilde{z}} = \tilde{a} \quad (40)$$

##### B. Circular trajectory

To derive linear dynamics about the circular trajectory, the Euler angle rates  $\dot{\tilde{\mu}}$  and  $\dot{\tilde{\nu}}$  are treated as control inputs. By solving the time derivative of equation (21), it becomes possible to calculate  $(\dot{\tilde{\beta}}, \dot{\tilde{\gamma}})$ . Subsequently, these values can be transformed into the true inputs  $(\tilde{\omega}_x, \tilde{\omega}_y, \tilde{\omega}_z)$  using Equation (7).

Unlike a fixed nominal position, the dynamics on a circular trajectory are not independent. The linearized equations of motion can be demonstrated to be as follows

$$\begin{aligned} \ddot{\tilde{p}} = \frac{\zeta_0^2}{L^2} \left[ \tilde{p} \left( \Omega^2 + \frac{gL^2}{\zeta_0^3} \right) + 2\dot{\tilde{q}}\Omega + \tilde{\mu} \left( -\frac{p_0}{\zeta_0} a_0 \sin \mu_0 - a_0 \cos \mu_0 \right) \right. \\ \left. + \tilde{a} \left( -\frac{p_0}{\zeta_0} \cos \mu_0 - \sin \mu_0 \right) \right] \end{aligned} \quad (41)$$

$$\ddot{\tilde{q}} = \tilde{q} \left( \Omega^2 + \frac{g}{\zeta_0} \right) - 2\dot{\tilde{p}}\Omega + \tilde{\nu} a_0 \quad (42)$$

$$\ddot{\tilde{u}} = \tilde{a} \sin \mu_0 + \tilde{\mu} a_0 \cos \mu_0 + 2\dot{\tilde{\nu}}\Omega + \tilde{u}\Omega^2 \quad (43)$$

$$\ddot{\tilde{v}} = -\tilde{\nu} a_0 - 2\dot{\tilde{u}}\Omega + \tilde{v}\Omega^2 \quad (44)$$

$$\ddot{\tilde{\omega}} = \tilde{a} \cos \mu_0 - \tilde{\mu} a_0 \sin \mu_0 \quad (45)$$

The linearized dynamics in the coordinate system C and W are observed to be time-invariant. The equations mentioned above simplify to Equations (34) - (40) when  $R = 0$  and  $\Omega = 0$ . When  $R = 0$ ,  $\Omega$  is a free parameter (see Equation (33)), allowing the description of the dynamics (34) - (40) in a rotating coordinate system.

## V. CONTROLLER DESIGN

We design linear full state feedback controller to stabilize the system about its nominal trajectories. It is used a Model Predictive Control (MPC) design. MPC is an optimal control strategy, i.e., based on numerical optimization. Depending on current measurements and prediction of future values of the output MPC calculations are done. The aim of the MPC control calculations is to find a successive control moves, which is the input i.e., called as manipulated input, so that the predicted response moves to the benchmark or set point in an optimal manner.

For implementation of the two mode (“Constant position” and “Circular trajectory”), the control strategy shall minimize at each step the difference between actual states and nominal states.

The nominal states are computed by equations shown in Par.III (Nominal trajectories).

The control strategy for both mode is implemented as follows:

$$\min_z x_N^T P x_N + \sum_{k=0}^{N-1} x_k^T Q x_k + u_k^T R u_k \quad (46)$$

$$\text{s.t.} : \begin{cases} u_{min} \leq u_k \leq u_{max} & \forall k = 0, 1, \dots, N-1 \\ y_{min} \leq y_k \leq y_{max} & \forall k = 0, 1, \dots, N-1 \\ x_{k+1} = A x_k + B u_k \\ x_0 = x(t) \end{cases} \quad (47)$$

For the implementation it is used a different form of this optimization problem that is a quadratic linear form and it is implemented as shown:

$$J(z, x_0) = \frac{1}{2} x_0^T Y x_0 + \min_z \frac{1}{2} z^T H z + z^T F x_0 \quad (48)$$

$$\text{s.t.} : \begin{cases} u_{min} \leq u_k \leq u_{max} & \forall k = 0, 1, \dots, N-1 \\ G z \leq W + S x_0 \end{cases} \quad (49)$$

The matrices  $H$ ,  $F$  and  $Y$  depends by weights matrices  $Q$ ,  $R$  and  $P$  by these equations:

$$Y = 2(\bar{Q} + \bar{T}^T \bar{Q} \bar{T}) \quad (50)$$

$$H = 2(\bar{R} + \bar{S}^T \bar{Q} \bar{S}) \quad (51)$$

$$F = 2(\bar{S}^T \bar{Q} \bar{T}) \quad (52)$$

The matrices  $\bar{Q}$  and  $\bar{R}$  are:

$$\bar{Q} = \begin{pmatrix} Q & 0 & \dots & 0 \\ 0 & Q & \dots & 0 \\ \vdots & \vdots & \ddots & \vdots \\ 0 & 0 & \dots & P \end{pmatrix} \quad (53)$$

$$\bar{R} = \begin{pmatrix} R & 0 & \dots & 0 \\ 0 & R & \dots & 0 \\ \vdots & \vdots & \ddots & \vdots \\ 0 & 0 & \dots & R \end{pmatrix} \quad (54)$$

The matrix  $\bar{S}$  is:

$$\bar{S} = \begin{pmatrix} B & 0 & \dots & 0 \\ AB & B & \dots & 0 \\ \vdots & \vdots & \ddots & \vdots \\ A^{N-1}B & A^{N-2}B & \dots & B \end{pmatrix} \quad (55)$$

The vector  $\bar{T}$  is:

$$\bar{T} = \begin{pmatrix} A \\ A^2 \\ \vdots \\ A^N \end{pmatrix} \quad (56)$$

The matrix  $G$  and  $S$  of the constraint are:

$$G = \begin{pmatrix} CB & 0 & \dots & 0 \\ CAB & CB & \dots & 0 \\ \vdots & \vdots & \ddots & \vdots \\ CA^{N-1}B & CA^{N-2}B & \dots & CB \end{pmatrix} \quad (57)$$

$$S = \begin{pmatrix} CA \\ CA^2 \\ \vdots \\ CA^N \end{pmatrix} \quad (58)$$

while the vector  $W$  is a vector of minimum/maximum limit of the states. The limits of the states, the matrices  $Q$  and  $R$  are grades of freedom and so they are chosen appropriately for both execution mode.

### A. Constant position

In this mode, the scope is to stabilize the pendulum on the quadrotor remaining in a constant position.

The position to be maintained has been choice in the origin so the linearization was made for each simulation step in the equilibrium point.

So the control strategy shall minimize at each step the difference between actual states and nominal states (shown in Par.III-A) that is computing considering reference by following is equal to zero.

The weights matrix  $Q$ ,  $R$  and the constraints are chosen with trial and error method. These parameters chosen and the limits of inputs and states are shown in Tab.I.

Control inputs	$[\omega_x, \omega_y, \omega_z, a]$
States	$[r, \dot{r}, x, \dot{x}, \beta, \dot{\beta}, s, \dot{s}, y, \dot{y}, \gamma, \dot{\gamma}, z, \dot{z}, \alpha, \dot{\alpha}]$
Input constraints	
Minimum u	$[-3, -1.5, -0.5, -13]$
Maximum u	$[3, 1.5, 0.5, 13]$
Outputs constraints	
Minimum x	$[-0.386, -2, -3.5, -7, -1.3, -7, -0.386, -2, -3.5, -7, -1.3, -7, -3.5, -7, -1.3, -7]$
Maximum x	$[0.386, 2, 3.5, 7, 1.3, 7, 0.386, 2, 3.5, 7, 1.3, 7, 3.5, 7, 1.3, 7]$
Prediction Horizon N	18
Simulation Steps T	60
Control Horizon	3
Q matrix	$10 * I(16)$
R matrix	$0.1 * I(4)$

Table I: Parameters of “Constant position” used in MPC.

### B. Circular trajectory

This problem is a tracking problem. The reference trajectory to be followed is a circular path. The simulation of the tracking of circular trajectory occurs in 60 steps so the trajectory is discretized by 60 points.

The equations of the dynamic system at each step are written in terms of deviations of the states (indicated by tilde).

For follow the trajectory the control strategy shall minimize these deviations and so the errors between actual states and nominal states that is the one of the reference trajectory.

The nominal states are computed during the linearization.

In this case, the linearization of the system is made for every point of the circular trajectory and so at each step we have a new equilibrium point.

The linearization is carried out by computing nominal states through formulae shown before (par.III-B) that concern the following of circular trajectory.

Then we update the matrices  $A$  and  $B$  of the system.

The weights matrix  $Q$ ,  $R$  and the constraints are chosen with trial and error method.

These parameters chosen and the limits of inputs and states are shown in Tab.II.

## VI. SIMULATION RESULTS

We have developed linear controllers for stabilizing a pendulum on a quadrotor, which can be applied to both static and dynamic equilibria of the pendulum.

From the simulation we can see that the results obtained by using the MPC controller for Constant position and Circular trajectory are congruent with respect to the desired ones: for the first case, it is obtained that the pendulum is stabilized on the quadrotor doing small motions, while in the second case, moreover stabilizing of the pendulum, the quadrotor follows a circular trajectory.

For the “Constant position” mode, some simulations were performed to estimate the maximum initial pendulum angle of inclination, considering as initial conditions of the drone it is stationary in the origin, which the drone fails to stabilize the pendulum and falls.

Control inputs	$[\dot{\mu}, \dot{\nu}, a]$
States	$[p, \dot{p}, q, \dot{q}, u, \dot{u}, v, \dot{v}, w, \dot{w}, \mu, \nu]$
Input constraints	
Minimum u	$[-3, -1.5, -13]$
Maximum u	$[3, 1.5, 13]$
States constraints	
Minimum x	$[-0.386, -2, -0.386, -2, -3.5, -7, -3.5, -7, -3.5, -7, -1.3, -1.3]$
Maximum x	$[0.386, 2, 0.386, 2, 3.5, 7, 3.5, 7, 3.5, 7, 1.3, 1.3]$
Prediction Horizon N	18
Simulation Steps T	60
Control Horizon	3
Q matrix	$Q = I(12); \quad Q(5, 5) = Q(7, 7) = Q(9, 9) = 10$
R matrix	$0.1 * I(3)$

Table II: Parameters of “Circular trajectory” used in MPC.

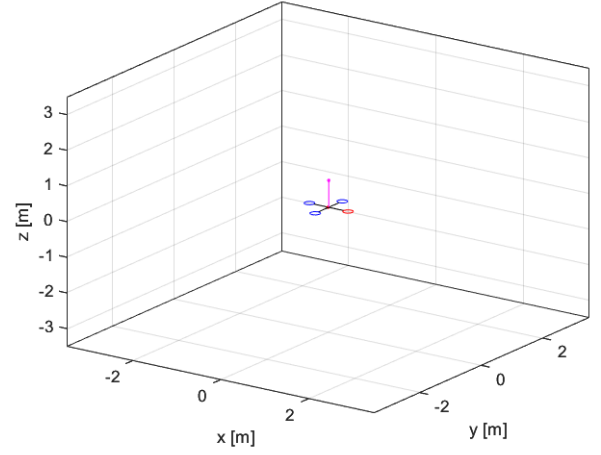


Figure 3: Final configuration of the simulation of “Constant position”. (The system is on the equilibrium point).

This calculated inclination angle is 46.5 which corresponds to the values of  $r$  and  $s$  equal to 0.29m. Through some trigonometric considerations and knowing  $L$  (length of the pendulum),  $\zeta$  (from Eq.(8)), the angle was calculated from the  $r$  and  $s$  states. The results are shown in Fig.3.

For the “Circular trajectory” mode, from the simulation it can be seen (Fig.4) the quadrotor initially does not follow the circular trajectory perfectly but travels a wider curve, but after about half the number of steps it follows the reference trajectory almost perfectly. This is shown in Fig.5. The pendulum is always well stabilized throughout the trajectory followed.

Future development consists in an experimental validation of controllers for standstill and circular motion to demonstrate their effectiveness in stabilizing the pendulum. Moreover, it is important to consider that the equations of motion used for deriving nominal trajectories and linear models neglect real world effects such as drag and underlying dynamics of the control inputs.

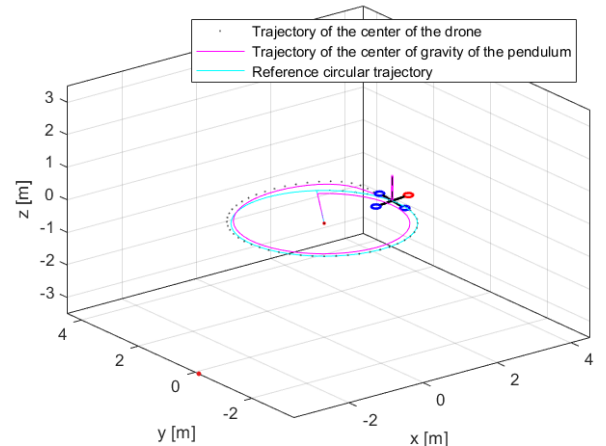


Figure 4: Reference circular trajectory, trajectory of the center of gravity of the pendulum, trajectory of the center of drone.

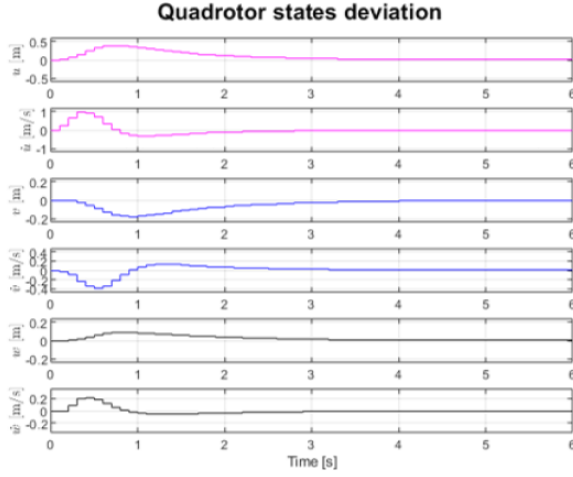


Figure 5: Drone's states deviations graphs in "Circular trajectory" simulation.

## VII. CONCLUSION AND OUTLOOK

We have developed linear controllers for stabilizing a pendulum on a quadrotor, which can be used for both static and dynamic equilibria of the pendulum. The virtual body frame is a useful tool to describe motions in a convenient coordinate system without enforcing this rotation for the vehicle.

Using its properties and a rotating coordinate system, the system description is time-invariant on circular trajectories.

Controllers for standstill and circular motion have not been validated experimentally and so this could be a possible improvement for the future.

Other ideas of possible future improvements are:

- implement the control strategy, obtained in simulation, in real environment;
- compare the simulated results with real experiments;
- add disturbances on the system and test the behaviors of the control strategy;
- analyze battery life cycle during the system's work.

## REFERENCES

- [1] Bertsekas, Dimitri P. (2007), *Dynamic Programming and Optimal Control*, vol. 2., Athena Scientific.
- [2] Borrelli, Francesco, Bemporad, Alberto, Morari, Manfred (2017), *Predictive control for linear and hybrid systems*, Cambridge University Press.
- [3] Ganga, G., Dharmana, Meher Madhu (2017) "MPC Controller for Trajectory Tracking Control of Quadcopter", IEEE, Int. Conf. on International Conference on circuits Power and Computing Technologies (ICCPCT), DOI: 10.1109/ICCPCT.2017.8074380.
- [4] Glielmo, Luigi (2023), *An Introduction to Optimization*, lecture slides.
- [5] Hehn, Markus, D'Andrea, Raffaello (2011), "A flying inverted pendulum", IEEE, Int. Conf. on International Conference on Robotics and Automation (ICRA), DOI: 10.1109/ICRA.2011.5980244.
- [6] Siciliano, Bruno, Sciavicco, Lorenzo, Villani, Luigi, Oriolo, Giuseppe (2008), *Robotica. Modellistica, pianificazione e controllo*, New York, McGraw-Hill Education.
- [7] Stama, Alfredo (2019), *Modellazione matematica e simulazione del sistema di controllo di un drone*. [Tesi di laurea triennale]. Ancona: Università Politecnica delle Marche.
- [8] [www.cvxr.com].
- [9] [www.researchgate.net/figure/Movement-of-quadcopter-body-frame-and-inertial-quadcopter-frame-3-Result-and-Discussion\_fig\_335719947].